

Microwave flux-flow Hall effect in a multi-band superconductor FeSe

R. Ogawa, F. Nabeshima and A. Maeda

*Department of Basic Science, The University of Tokyo,
3-8-1 Komaba, Meguro-ku, Tokyo 153-8902, Japan*

We measured the flux-flow Hall effect in a multi-band superconductor FeSe pure single crystal to investigate the nature of the vortex core state by means of the cross-shaped bimodal cavity technique. We found that the flux-flow Hall angle of FeSe is about 0.5 at low temperatures, which is equal to or smaller than that evaluated by the effective viscous drag coefficient measurements, and the Hall angle, as a function of the magnetic field, behaves in a different manner from the viscous drag coefficient measurements. These features contrast the cuprate superconductors. The conductivity tensor of multi-band superconductors that are contributed from holes and electrons explains the observed behaviors. This means that the observed results are due to partial cancellation of the flux-flow Hall voltage by the electrons and holes. Therefore, our study is the first demonstration of a novel feature characteristic of flux flow in multi-band superconductors.

I. INTRODUCTION

Quasiparticles (QPs) are confined and form quantized energy levels in a vortex core [1]. The energies of the quantized levels are expressed as $E_N = \Delta E(N + 1/2)$, where $\Delta E \equiv \hbar\omega_0 = \hbar\Delta_0^2/E_F$ (Δ_0 and E_F are the superconducting gap and Fermi energy) is the level spacing, and N is an integer. Because each level has some width $\delta E = \hbar/\tau$, the ratio of the energy spacing to its width, $r \equiv \Delta E/\delta E = \omega_0\tau$, represents the degree of quantized nature of the vortex core. In the limit $r \gg 1$, the quantized nature inside the core is distinct, while in the opposite limit $r \ll 1$, the core can be regarded as a normal metal. For an r value between the two limits, the vortex core is called moderately clean, where the quantized nature is marginal. As the quantized core is expected to represent many novel features, it is extremely important to know the r value. In fact, parameter r is deeply correlated with the dynamics of vortices. Based on the conventional understanding [2], when an external driving current $\mathbf{J} = (J_0, 0)$ is applied in the x - y plane to a superconductor under a magnetic field in the z direction, the driving force $\Phi_0\mathbf{J} \times \hat{z}$ forces a vortex, whose displacement is $\mathbf{u} = (x, y)$, to move in a certain direction with an angle $\phi = \tan^{-1}(\dot{y}/\dot{x})$, generating an electric field \mathbf{E} , where $\Phi_0 = h/2e$ is the flux quantum, and \hat{z} is a unit vector in the z direction. When we can neglect the influence of pinning, the equation of motion of a vortex is as follows:

$$\Phi_0\mathbf{J} \times \hat{z} = \eta\dot{\mathbf{u}} + \alpha_H\dot{\mathbf{u}} \times \hat{z}, \quad (1)$$

where $\eta = \pi\hbar nr/(1+r^2)$ is the viscous drag coefficient in the longitudinal direction, $\alpha_H = \pi\hbar nr^2/(1+r^2)$ is the viscous drag coefficient in the transvers direction, and n is the density of QPs. Solving the equation of motion yields the flux-flow Hall angle:

$$\tan\theta \equiv \tan(\phi - \frac{\pi}{2}) = \frac{\alpha_H}{\eta} = r. \quad (2)$$

On the other hand, under a constant current, the flux-flow resistivity ρ_f relates to the effective viscous drag coefficient as $\eta_{eff} = \Phi_0 B/\rho_f$ [3, 4], and r can also be

represented in terms of η_{eff} as

$$\eta_{eff} \equiv \eta \left(1 + \frac{\alpha_H^2}{\eta^2} \right) = \pi\hbar nr. \quad (3)$$

Both the measurements of the flux-flow resistivity ρ_f and flux-flow Hall angle θ can provide information about the QPs state in the vortex core. Thus, we can choose either of the two methods: (1) the flux-flow Hall angle measurement or (2) the effective viscous drag coefficient measurement. So far, the latter approach has been commonly considered owing to the ease of experimentation [5, 6]. To obtain information about r , we need the values of viscous drag coefficients at sufficiently low temperatures, well below the superconducting transition temperature T_c , which is unachievable by an ordinary DC resistivity measurement because of pinning. Note that we measured the DC Hall resistivity of FeSe $_x$ Te $_{1-x}$ films in the mixed state near T_c and found that the sign reversal of the DC Hall voltage appears often possibly due to pinning [7]. Therefore, even near T_c , the effect of pinning cannot be neglected in DC measurements. Thus, high frequency measurements (typically microwave) [8] and/or the analysis of the data by a reliable model that can obtain the value of viscous drag coefficients from the measured data [9] are necessary.

High- T_c cuprates are among the most promising candidate materials for the quantized core due to their large energy gap and small Fermi energy. Thus, we investigated flux flow by using microwaves and obtained several interesting but puzzling features. In the η_{eff} measurement, it was found that the core in motion was moderately clean ($\omega_0\tau \sim 0.1-0.3$) for a wide range of materials, independent of the cleanness of the core [4, 10–12]. However, during the direct Hall angle measurement using the microwave techniques developed by us [13], we found that $\omega_0\tau \sim 1-3$ for both Bi $_2$ Sr $_2$ CaCu $_2$ O $_y$ and YBa $_2$ Cu $_3$ O $_y$, which are larger by an order of magnitude than those evaluated using the η_{eff} measurement, and rather close to the originally expected value of r [14]. We explain the origin of the discrepancy in terms of the non-linearity in the viscous drag coefficient [15] and other possible dissipation mechanisms for the moving vortex that are not

represented by the basic equation of motion of the vortex, including those recently proposed [16–19]. However, it is not known whether such a large value and the discrepancy between the two methods will be observed in other clean superconductors.

FeSe is another promising candidate for the quantized core because of its very small Fermi energy, comparable to the superconducting gap $\Delta_0 \sim E_F$ [20], and long QP-lifetime τ in the superconducting state [21]. Indeed, scanning tunneling spectroscopy (STS) measurements of FeSe single crystals show Friedel-like oscillations, which shows the quantized levels in the core [22], and we expect that features specific to superclean cores will be observed. The η_{eff} measurement of a pure single crystal of FeSe yields $r = 1 \pm 0.5$ [21]. Although this is the largest value of r measured thus far among various superconductors, it is still in the moderate clean region. We expect a much larger value in flux-flow Hall angle measurements. Another interesting viewpoint is that FeSe is a multi-band superconductor, where we expect to observe novel effects. Indeed, in multi-band superconductors, the dissociation of electron and hole vortices has been proposed theoretically [23]. Although there have been experimental studies to investigate flux flow in multi-band superconductors [21, 24–31], no such novel feature has been reported.

In this study, we investigated the microwave flux-flow Hall effect in FeSe pure single crystals using the cross-shaped bimodal cavity technique. We find that the flux-flow Hall angle of FeSe is about 0.5 at low temperatures, which is equal to or smaller than that evaluated by the η_{eff} measurement. In addition, the Hall angle behaves in a different manner as a function of the magnetic field from what was obtained from the η_{eff} measurement. These features contrast the cuprate superconductors. We argue that these might be characteristic of multi-band superconductors due to the cancellation of contributions from the hole and the electron. Therefore, our study is the first demonstration of novel feature characteristics of flux flow in multi-band superconductors.

II. METHODS

The magnitude of the flux-flow Hall angle is given by $|\tan \theta| = |E_y/E_x|$ from Faraday’s law $\mathbf{E} = \dot{\mathbf{u}} \times \mathbf{B}$. The definition of the surface impedance tensor is $\tilde{Z} \equiv \mathbf{E}^{\parallel}(z = 0)/\int_0^{\infty} \mathbf{J} dz$, which yields $\mathbf{E} \propto \tilde{Z} \mathbf{J}$, where the symbol \parallel indicates that it is parallel to the surface of the sample. Thus, the magnitude of the flux-flow Hall angle is represented as

$$|\tan \theta| = \left| \frac{\sigma_{xy}}{\sigma_{xx}} \right| = \left| \frac{Z^H}{Z^L} \right|, \quad (4)$$

where σ_{xx} and σ_{xy} are the longitudinal and transverse conductivities, respectively, and Z^L and Z^H are the diagonal and off-diagonal components of the surface

impedance tensor, respectively [13]. Three types of measurements are necessary to obtain the magnitude of the flux-flow Hall angle: the DC resistivity measurements, measurements of the longitudinal components of the surface impedance tensor, Z^L , and measurements of the transverse components of the surface impedance tensor, Z^H . The DC resistivity tensor $\tilde{\rho}$ is measured using a Physical Property Measurement System (PPMS) from Quantum Design in a standard six-probe configuration. The longitudinal components of the surface impedances tensor Z^L are measured using the conventional cavity perturbation method with a cylindrical cavity [5], whereas the transverse components of the surface impedances tensor Z^H are measured using a cross-shaped bimodal cavity, in which the changes in the resonance characteristics and the surface impedance tensor of the sample are represented as

$$\Delta \left(\frac{1}{2Q} \right) = \Delta (G^L R^L + G^H |X^H|) \quad (5)$$

and

$$\Delta \left(\frac{f}{f_0} \right) \equiv -\frac{f - f_0}{f_0} = \Delta (G^L X^L - G^H |R^H|), \quad (6)$$

where Q denotes the quality factor of the resonance, f and f_0 denote the resonance frequencies with and without the sample, respectively, R^L and X^L are the real and imaginary parts of the longitudinal components of the surface impedance tensor ($Z^L \equiv R^L - iX^L$), respectively, R^H and X^H are the real and imaginary parts of the transverse components of the surface impedance tensor ($Z^H \equiv R^H - iX^H$), respectively, G^L and G^H represent the geometric constants in the longitudinal and transverse directions, respectively, which depend on the shape of the cavity and the sample and take the same value under the assumption that these geometries are symmetrical ($G^L = G^H$), and Δ represents the difference between the data of the same sample at different temperatures. For explicit procedure, see ref. [13].

FeSe pure single crystals were synthesized by the chemical vapor transport technique in a temperature gradient furnace using KCl/AlCl₃ flux [32]. We performed the microwave measurements using the cross shaped bimodal cavity, operating in the two orthogonal TE₀₁₁ and TE₁₀₁ modes at 15.8 GHz, which have a quality factor Q of approximately 3×10^3 . The sample sizes for the cross-shaped bimodal cavity measurements are typically $1.2 \times 1.2 \times 0.1$ mm³. In all experiments, magnetic fields of up to 7 T were applied under field-cooled conditions.

III. RESULTS AND DISCUSSION

Figures 1(a) and (b) show the temperature dependence of the DC longitudinal resistivity ρ_{xx} of FeSe. T_c^{zero} is about 9 K and residual resistivity ratio ($RRR = \rho_{xx}(300 \text{ K})/\rho_{xx}(T_c^{onset} = 10 \text{ K})$) is about 29. Figure 1(c)

shows the magnetic field dependence of the DC Hall angle $\tan\theta_{dc}$ in the normal state. The DC Hall angle of FeSe single crystal above T_c shows non-linearity with respect to the magnetic field due to its multi-carrier nature, as is well known [33]. Figure 2 shows the temperature dependence of the longitudinal components of the surface impedance tensor Z^L under the magnetic field. Z^L increases with an increasing magnetic field and decreases with a decreasing temperature. This behavior is in accordance with flux-flow resistivity [21]. Therefore, most of the observed behavior of Z_L can be attributed to flux-flow. These results demonstrate that the sample used for experiments has the usual properties of FeSe single crystals. Figure 3 shows the magnitude of the magnetic field dependence of the flux-flow Hall angle $|\tan\theta|$. The uncertainty is mainly due to the small signal (change in the resonance characteristics) of the sample. It increases with decreasing temperature due to the development of a superconducting condensate in small magnetic fields. We observed that the magnitude of the flux-flow Hall angle at 5.3 K is about 0.5. It is equal to or slightly smaller than that evaluated from the effective viscous drag coefficient measurement ($r = 1.0 \pm 0.5$) [21]. The flux-flow Hall angle does not depend on magnetic field strongly, even showing a very weak magnetic field dependence. This field dependence is rather different from what was observed in the η_{eff} measurement, where it increases with increasing magnetic field as $\tan\theta \sim B^{0.2}$, corresponding to the sublinear increase of the flux-flow resistivity as a function of magnetic field.

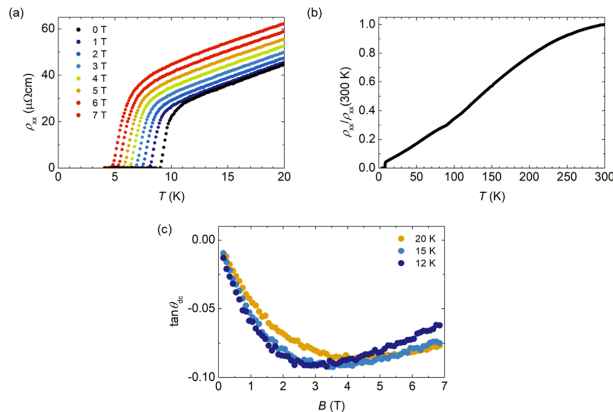


FIG. 1. (a) The temperature dependence of the longitudinal resistivity of FeSe under a magnetic field near T_c (b) The temperature dependence of the normalized longitudinal resistivity $\rho_{xx}/\rho_{xx}(300\text{ K})$ at 0 T; T_c^{zero} is about 9 K and $RRR = \rho_{xx}(300\text{ K})/\rho_{xx}(T_c^{onset} = 10\text{ K})$ is about 29 (c) The magnetic field dependence of the DC Hall angle $\tan\theta_{dc}$ in the normal state (20 K, 15 K, and 12 K, respectively). The Hall angle behaves non-monotonically with an increasing magnetic field due to its multi-carrier nature.

The result of the flux-flow Hall effect in FeSe is remarkable in two senses. (1) Unlike cuprate superconductors, the magnitude of the flux-flow Hall angle is equal to or smaller than that evaluated from η_{eff} . (2) There is a

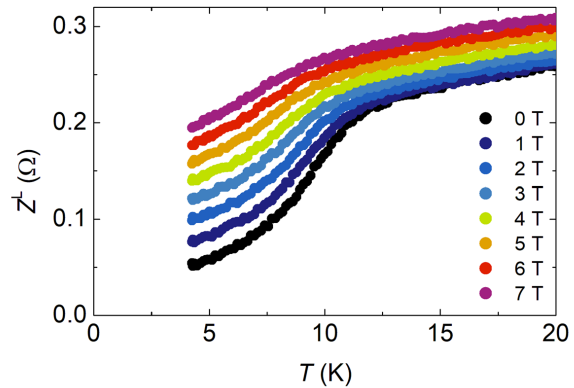


FIG. 2. Temperature dependence of the longitudinal components of the surface impedance tensor Z^L ; magnetic fields of up to 7 T are applied under field-cooled conditions.

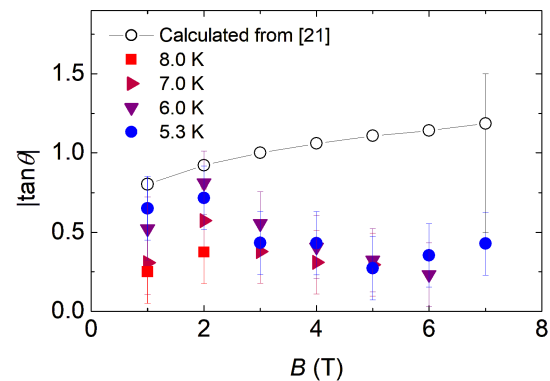


FIG. 3. Magnetic field dependence of the magnitude of the flux-flow Hall angle $|\tan\theta|$; magnetic fields of up to 7 T are applied under field-cooled conditions. Open circles indicate the flux-flow Hall angle calculated from the data of η_{eff} measurements [21]. The magnitude of flux-flow Hall angle at low temperatures is equal to or smaller than that evaluated from the effective viscous drag coefficient and does not depend on magnetic-field strongly even showing a very weak field dependence, which are different from η_{eff} measurements.

discrepancy in the magnetic field dependence of the Hall angle between the direct Hall angle measurement and the η_{eff} measurement in the same material. To understand the first feature, we consider that the multi-band nature of FeSe is essentially important. FeSe has two hole bands at the Γ point and two electron bands at the M point [34]. Both holes and electrons contribute to DC transport properties in the normal state, leading to a cancellation of the Hall voltage [33]. We believe that a similar effect can take place even in vortex dynamics. However, except for DC measurements in the vicinity of T_c [7, 35–37], no direct observation of the flux-flow Hall effect in multi-band superconductors well below T_c has been reported in experiments. On the other hand, the-

oretical studies of vortex dynamics in multi-band superconductors have been undertaken [23, 39, 40]. In particular, a microscopic theory [38] shows that the flux-flow conductivity tensor has contributions from holes as well as electrons. We believe that the competition of these contributions can explain the difference in the estimated number of Hall angle between the two methods in both the magnitude. Below we will discuss this scenario more explicitly.

According to the microscopic theory[38], in the flux-flow regime, vortex dynamics is dominated by the force balance equation $f_L + f_{env} = 0$, where f_L is the Lorentz force due to the external transport current and f_{env} is the environmental force. The environmental force originates from the environment on a vortex (e.g., Magnus force, spectral force, *etc.*) and is expressed as a linear superposition of terms contributed by the different bands, k such that $f_{env} = \sum_k f_k$. Therefore, for FeSe where both hole bands and electron bands contribute, the flux-flow conductivity tensor also has contributions from holes as well as electrons, and these contributions cause cancellations in the off-diagonal components (Hall components). On the other hand, in the diagonal components, both contribute additively. Explicitly, the expressions for flux-flow conductivity in the longitudinal and transverse directions at low temperatures are as follows.

$$\sigma_{xx} = \frac{2e}{(2\pi)^3 B} \sum_n \left(\int_e + \int_h \right) S(p_z) dp_z \times \int \frac{db}{2} \frac{\partial \epsilon_n}{\partial b} \frac{df^{(0)}(\epsilon_n)}{d\epsilon} \gamma_{xx}(\epsilon_n), \quad (7)$$

$$\sigma_{xy} = \frac{2e}{(2\pi)^3 B} \sum_n \left(\int_e - \int_h \right) S(p_z) dp_z \times \int \frac{db}{2} \frac{\partial \epsilon_n}{\partial b} \frac{df^{(0)}(\epsilon_n)}{d\epsilon} \gamma_{xy}(\epsilon_n), \quad (8)$$

where p_z denotes the momentum along the z axis, $S(p_z)$ denotes the area of the cross section of the Fermi surface cut by the plane $p_z = const$, b denotes the impact factor, ϵ_n denotes the energy spectrum, n denotes an index for the energy spectrum, $f^{(0)}$ denotes the equilibrium distribution function, and $\gamma_{xx(xy)}$ are the factors defined by ω_n and τ_n , which are an energy-interval spacing and relaxation time, as $\gamma_{xx}(\epsilon_n) = \omega_n \tau_n / (1 + \omega_n^2 \tau_n^2)$ and $\gamma_{xy}(\epsilon_n) = \omega_n^2 \tau_n^2 / (1 + \omega_n^2 \tau_n^2)$, respectively. We write these equations as $\sigma_{xx} = e\Gamma_x(N_e + N_h)/B$ and $\sigma_{xy} = e\Gamma_y(N_e - N_h)/B$, where N_e and N_h are the density of electrons and holes, respectively, and Γ_x and Γ_y are coefficients which represent other factors, respectively. By defining the ratio of the contributions of holes to those of electrons as $\beta \equiv N_h/N_e$ and $e\Gamma_{x(y)} \equiv D_{x(y)}$, we obtain that $\sigma_{xx} = D_x N_e (1 + \beta)/B$ and $\sigma_{xy} = D_y N_e (1 - \beta)B$. With these notations, the experimentally evaluated value of the degree of quantization (DQ) by the $\tan\theta$ measurement, r_H , and that by the η_{eff} measurement, r_η , are

expressed as

$$r_H = \left| \frac{\sigma_{xy}}{\sigma_{xx}} \right| = \left| \frac{D_y(1 - \beta)}{D_x(1 + \beta)} \right| \quad (9)$$

and

$$r_\eta = \frac{B\Phi_0}{\pi\hbar n} \cdot \sigma_{xx} \left[1 + \left(\frac{\sigma_{xy}}{\sigma_{xx}} \right)^2 \right] = \frac{\Phi_0}{\pi\hbar} \cdot D_x \left[1 + \left(\frac{D_y(1 - \beta)}{D_x(1 + \beta)} \right)^2 \right], \quad (10)$$

respectively.

To see the ‘‘complicated’’ interaction of electron bands and hole bands, we change β and investigate how r_H and r_η behave explicitly, which is represented in figure 4(a). Note that the data is normalized by the value at $\beta = 0$ (corresponding to a single-band case). In figure 4(a), $\tilde{r}_H - \tilde{r}_\eta \equiv r_H(\beta)/r_H(0) - r_\eta(\beta)/r_\eta(0)$ are shown for the various value of D_y/D_x . We find that $\tilde{r}_H - \tilde{r}_\eta$ is negative in wide range of regions, except in the vicinity of $\beta = 0$. This means that the DQs evaluated by $\tan\theta$ measurements are smaller than those evaluated by η_{eff} measurements, rather generally for materials having both electron bands and hole bands. This is in good agreement with what we observed in FeSe.

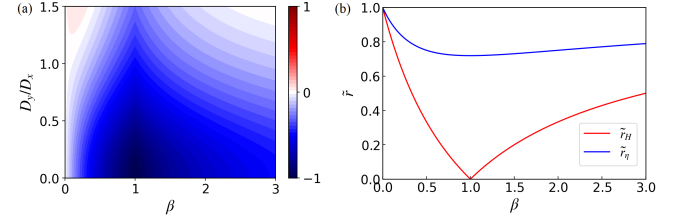


FIG. 4. (a) Contours of $\tilde{r}_H - \tilde{r}_\eta$. In the blue colored region, \tilde{r}_H is smaller than \tilde{r}_η . (b) The β dependence of the normalized DQs \tilde{r}_H and \tilde{r}_η when $D_y/D_x = 5/8$; the red lines represent values obtained from $\tan\theta$ measurements \tilde{r}_H , and the blue lines represent those obtained from η_{eff} measurements \tilde{r}_η . Fig. 4(b) corresponds to the cross-section of Fig. 4(a) at $D_y/D_x = 5/8$. \tilde{r}_H is always smaller than \tilde{r}_η except for β is 0.

Next, we will discuss the above mentioned scenario more quantitatively, and try to extract some numbers for parameters shown up above. For that purpose, it should be noted that both Γ_x and Γ_y depend on purity of superconductors. At low temperatures and for small magnetic fields limit, when $\omega_0\tau \approx 1$, explicit calculation of eqs. (7) and (8) leads to $\Gamma_x \approx 0.8$ and $\Gamma_y \approx 0.5$ [38]. Soon below, we will reestimate Γ_x and Γ_y from the experimental data, and check the consistency of the choice, $\Gamma_y/\Gamma_x = D_y/D_x = 5/8$. With $D_y/D_x = 5/8$,

$$r_H = \frac{5}{8} \cdot \left| \frac{1 - \beta}{1 + \beta} \right| \quad (11)$$

and

$$r_\eta = \frac{\Phi_0}{\pi\hbar} \cdot D_x \left[1 + \left(\frac{5}{8} \cdot \frac{1 - \beta}{1 + \beta} \right)^2 \right]. \quad (12)$$

Figure 4(b) shows the β dependence of the normalized DQs \tilde{r}_H and \tilde{r}_η when D_x/D_y equals to 5/8. In particular, for $\beta = 1$, the magnitudes of the electron and hole contributions are exactly the same, so $\tilde{r}_H = 0$ due to the oppositely acting contribution of electrons and holes. From eq. (11), we can calculate that $\beta \approx 0.11$ since $r_H \approx 0.5$ as shown in figure 3. This means that the magnitude of the contribution from, for instance, electrons is about one tenth of holes. (Since in our measurement, sign of the Hall coefficient cannot be obtained, the role of electrons and hole can be reversed). Substituting this value into eq. (12), we find that $r_\eta/D_x = 7.5 \times 10^{18} \text{ C}^{-1}$, leading to D_x is approximately $1.3 \times 10^{-19} \text{ C}$ with $r_\eta = 1.0$. This means $\Gamma_x \approx 0.83$ and $\Gamma_y \approx 0.52$, which is comparable to theoretically estimated value just above.

As for the magnetic field dependence of two DQs, β is considered not to show the strong magnetic field dependence since it only depends on the carrier density. The definition in eqs. (7) and (8) suggest that $D_{x(y)}$, namely $\Gamma_{x(y)}$, is considered not to show strong magnetic field dependence either. However, it should be noted that these equations were derived under the assumption that the order parameter is uniform (isotropic). Experiments found that superconducting gap of FeSe is highly anisotropic [20, 43]. Since in Fe-based superconductors

including FeSe, the sub-linear magnetic field dependence of the flux-flow resistivity obtained by η_{eff} study is closely related to the fact that the superconducting gap function is anisotropic [30, 44], we may expect that the anisotropy of superconducting gaps explains the difference in the magnetic-field dependence between r_H and r_η .

IV. CONCLUSION

In summary, we measured the flux-flow Hall effect in a multi-band superconductor FeSe pure single crystal to investigate the nature of the vortex core state by means of the cross-shaped bimodal cavity technique. We found that the flux-flow Hall angle of FeSe is about 0.5 at low temperatures, which is equal to or smaller than that evaluated by the η_{eff} measurements. We consider that the observed feature is related to the multi-band nature of FeSe. Our calculations for the flux-flow conductivity tensor for multi-band superconductors that has contributions from holes as well as electrons show partial cancellation of the flux-flow Hall voltage. Therefore, our study is the first demonstration of a novel feature characteristic of flux flow in multi-band superconductors.

-
- [1] C. Caroli, P. De Gennes, and J. Matricon, *Bound Fermion states on a vortex line in a type II superconductor*, Physics Letters **9**, 307 (1964).
- [2] G. Blatter, M. V. Feigel'man, V. B. Geshkenbein, A. I. Larkin, and V. M. Vinokur, *Vortices in high-temperature superconductors*, Reviews of Modern Physics **66**, 1125 (1994).
- [3] M. Golosovsky, M. Tsindlekht, and D. Davidov, *High-frequency vortex dynamics in $YBa_2Cu_3O_7$* , Superconductor Science and Technology **9**, 1 (1996).
- [4] Y. Tsuchiya, K. Iwaya, K. Kinoshita, T. Hanaguri, H. Kitano, A. Maeda, K. Shibata, T. Nishizaki, and N. Kobayashi, *Electronic state of vortices in $YBa_2Cu_3O_y$ investigated by complex surface impedance measurements*, Physical Review B **63**, 184517 (2001).
- [5] O. Klein, S. Donovan, M. Dressel, and G. Grüner, *Microwave cavity perturbation technique: Part I: Principles*, International Journal of Infrared and Millimeter Waves **14**, 2423 (1993).
- [6] M. Golosovsky, M. Tsindlekht, H. Chayet, and D. Davidov, *Vortex depinning frequency in $YBa_2Cu_3O_{7-x}$ superconducting thin films: Anisotropy and temperature dependence*, Physical Review B **50**, 470 (1994).
- [7] R. Ogawa, T. Ishikawa, M. Kawai, F. Nabeshima, and A. Maeda, *Direct Current Measurement of Hall Effect in the Mixed State for the Iron-chalcogenide Superconductors*, Journal of Physics: Conference Series **1054**, 012021 (2018).
- [8] J. I. Gittleman and B. Rosenblum, *The Pinning Potential and High-Frequency Studies of Type-II Superconductors*, Journal of Applied Physics **39**, 2617 (1968).
- [9] M. W. Coffey and J. R. Clem, *Unified theory of effects of vortex pinning and flux creep upon the rf surface impedance of type-II superconductors*, Physical Review Letters **67**, 386 (1991).
- [10] T. Hanaguri, T. Tsuboi, Y. Tsuchiya, K. Sasaki, and A. Maeda, *Reduction of the Superfluid Density in the Vortex-Liquid Phase of $Bi_2Sr_2CaCu_2O_y$* , Physical Review Letters **82**, 1273 (1999).
- [11] A. Maeda, H. Kitano, K. Kinoshita, T. Nishizaki, K. Shibata, and N. Kobayashi, *Effect of Nonmagnetic Impurities on the Electronic State of Quasiparticles Confined in the Naturally Prepared Nanostructure under Magnetic Field in $YBa_2Cu_3O_y$* , Journal of the Physical Society of Japan **76**, 094708 (2007).
- [12] A. Maeda, T. Umetsu, and H. Kitano, *Viscosity of quantized vortices of high- T_c superconductors, $La_{2-x}Sr_xCuO_4$ as a function of carrier concentration*, Physica C: Superconductivity **460-462**, 1202 (2007).
- [13] R. Ogawa, T. Okada, H. Takahashi, F. Nabeshima, and A. Maeda, *Microwave Hall effect measurement for materials in the skin depth region*, Journal of Applied Physics **129**, 015102 (2021).
- [14] R. Ogawa, F. Nabeshima, T. Nishizaki, and A. Maeda, *Large Hall angle of vortex motion in high- T_c cuprate superconductors revealed by microwave flux-flow Hall effect*, Physical Review B **104**, L020503 (2021).
- [15] A. Larkin and Y. Ovchinnikov, *Nonlinear conductivity of superconductors in the mixed state*, JETP **41**, 960 (1976).
- [16] S. Hofmann and R. Kümmel, *Moving vortex line: Electronic structure, Andreev scattering, and Magnus force*, Physical Review B **57**, 7904 (1998).

- [17] M. Hayashi, *Spectral Flow and Quantum Theory of Dissipation in the Vortex Core of BCS Superconductors*, Journal of the Physical Society of Japan **67**, 3372 (1998).
- [18] M. Smith, A. V. Andreev, M. V. Feigel'man, and B. Z. Spivak, *Conductivity of superconductors in the flux flow regime*, Physical Review B **102**, 180507 (2020).
- [19] V. G. Kogan and N. Nakagawa, *Current distributions by moving vortices in superconductors*, Physical Review B **103**, 134511 (2021).
- [20] S. Kasahara, T. Watashige, T. Hanaguri, Y. Kohsaka, T. Yamashita, Y. Shimoyama, Y. Mizukami, R. Endo, H. Ikeda, K. Aoyama, T. Terashima, S. Uji, T. Wolf, H. Von Löhneysen, T. Shibauchi, and Y. Matsuda, *Field-induced superconducting phase of FeSe in the BCS-BEC cross-over*, Proceedings of the National Academy of Sciences of the United States of America **111**, 16309 (2014).
- [21] T. Okada, Y. Imai, T. Urata, Y. Tanabe, K. Tanigaki, and A. Maeda, *Electronic States and Energy Dissipations of Vortex Core in Pure FeSe Single Crystals Investigated by Microwave Surface Impedance Measurements*, Journal of the Physical Society of Japan **90**, 094704 (2021).
- [22] T. Hanaguri, S. Kasahara, J. Böker, I. Eremin, T. Shibauchi, and Y. Matsuda, *Quantum Vortex Core and Missing Pseudogap in the Multiband BCS-BEC Crossover Superconductor FeSe*, Physical Review Letters **122**, 077001 (2019).
- [23] S.-Z. Lin and L. N. Bulaevskii, *Dissociation Transition of a Composite Lattice of Magnetic Vortices in the Flux-Flow Regime of Two-Band Superconductors*, Physical Review Letters **110**, 087003 (2013).
- [24] A. Shibata, M. Matsumoto, K. Izawa, Y. Matsuda, S. Lee, and S. Tajima, *Anomalous flux flow resistivity in the two-gap superconductor MgB₂*, Physical Review B **68**, 060501 (2003).
- [25] S. Akutagawa, T. Ohashi, H. Kitano, A. Maeda, J. Goryo, H. Matsukawa, and J. Akimitsu, *Quasiparticle Electronic Structure of a New Superconductor, Y₂C₃, in the Mixed State Investigated by Specific Heat and Flux-Flow Resistivity*, Journal of the Physical Society of Japan **77**, 064701 (2008).
- [26] T. Okada, H. Takahashi, Y. Imai, K. Kitagawa, K. Matsubayashi, Y. Uwatoko, and A. Maeda, *Microwave surface-impedance measurements of the electronic state and dissipation of magnetic vortices in superconducting LiFeAs single crystals*, Physical Review B **86**, 064516 (2012).
- [27] H. Takahashi, T. Okada, Y. Imai, K. Kitagawa, K. Matsubayashi, Y. Uwatoko, and A. Maeda, *Investigation of the superconducting gap structure in SrFe₂(As_{0.7}P_{0.3})₂ by magnetic penetration depth and flux flow resistivity analysis*, Physical Review B **86**, 144525 (2012).
- [28] T. Okada, H. Takahashi, Y. Imai, K. Kitagawa, K. Matsubayashi, Y. Uwatoko, and A. Maeda, *Low energy excitations inside the vortex core of LiFe(As, P) single crystals investigated by microwave-surface impedance*, Physica C: Superconductivity **484**, 27 (2013).
- [29] T. Okada, H. Takahashi, Y. Imai, K. Kitagawa, K. Matsubayashi, Y. Uwatoko, and A. Maeda, *Magnetic penetration depth and flux-flow resistivity measurements on NaFe_{0.97}Co_{0.03}As single crystals*, Physica C: Superconductivity **494**, 109 (2013).
- [30] T. Okada, Y. Imai, H. Takahashi, M. Nakajima, A. Iyo, H. Eisaki, and A. Maeda, *Penetration depth and flux-flow resistivity measurements of BaFe₂(As_{0.55}P_{0.45})₂ single crystals*, Physica C: Superconductivity and its Applications **504**, 24 (2014).
- [31] T. Okada, F. Nabeshima, H. Takahashi, Y. Imai, and A. Maeda, *Exceptional suppression of flux-flow resistivity in FeSe_{0.4}Te_{0.6} by back-flow from excess Fe/Te substitutions*, Physical Review B **91**, 054510 (2015).
- [32] A. E. Böhrer, F. Hardy, F. Eilers, D. Ernst, P. Adelmann, P. Schweiss, T. Wolf, and C. Meingast, *Lack of coupling between superconductivity and orthorhombic distortion in stoichiometric single-crystalline FeSe*, Physical Review B **87**, 180505 (2013).
- [33] H. Lei, D. Graf, R. Hu, H. Ryu, E. S. Choi, S. W. Tozer, and C. Petrovic, *Multiband effects on β -FeSe single crystals*, Physical Review B **85**, 094515 (2012).
- [34] A. Subedi, L. Zhang, D. J. Singh, and M. H. Du, *Density functional study of FeS, FeSe, and FeTe: Electronic structure, magnetism, phonons, and superconductivity*, Physical Review B **78**, 134514 (2008).
- [35] R. Jin, M. Paranthaman, H. Y. Zhai, H. M. Christen, D. K. Christen, and D. Mandrus, *Unusual Hall effect in superconducting MgB₂ films*, Physical Review B **64**, 220506 (2001).
- [36] H. Lei, R. Hu, E. S. Choi, and C. Petrovic, *Thermally activated energy and flux-flow Hall effect of Fe_{1+y}(Te_{1+x}S_x)_z*, Physical Review B **82**, 134525 (2010).
- [37] L. M. Wang, U.-C. Sou, H. C. Yang, L. J. Chang, C.-M. Cheng, K.-D. Tsuei, Y. Su, T. Wolf, and P. Adelmann, *Mixed-state Hall effect and flux pinning in Ba(Fe_{1-x}Co_x)₂As₂ single crystals ($x = 0.08$ and 0.10)*, Physical Review B **83**, 134506 (2011).
- [38] N. B. Kopnin, *Theory of nonequilibrium superconductivity*, Vol. 110 (Oxford University Press., 2001).
- [39] E. Babaev, *Vortices with Fractional Flux in Two-Gap Superconductors and in Extended Faddeev Model*, Physical Review Letters **89**, 067001 (2002).
- [40] M. Silaev and A. Vargunin, *Vortex motion and flux-flow resistivity in dirty multiband superconductors*, Physical Review B **94**, 1 (2016).
- [41] K. K. Huynh, Y. Tanabe, T. Urata, H. Oguro, S. Heguri, K. Watanabe, and T. Tanigaki, *Electric transport of a single-crystal iron chalcogenide FeSe superconductor: Evidence of symmetry-breakdown nematicity and additional ultrafast Dirac cone-like carriers*, Physical Review B **90**, 144516 (2014).
- [42] T. Terashima, N. Kikugawa, A. Kiswandhi, E.-S. Choi, J. S. Brooks, S. Kasahara, T. Watashige, H. Ikeda, T. Shibauchi, Y. Matsuda, T. Wolf, A. E. Böhrer, F. Hardy, C. Meingast, H. Löhneysen, M. Suzuki, R. Arita, and Y. Uji, *Anomalous Fermi surface in FeSe seen by Shubnikov-de Haas oscillation measurements*, Physical Review B **90**, 144517 (2014).
- [43] D. Liu, C. Li, J. Huang, B. Lei, L. Wang, X. Wu, B. Shen, Q. Gao, Y. Zhang, X. Liu, Y. Hu, A. Liang, J. Liu, P. Ai, L. Zhao, S. He, L. Yu, G. Liu, Y. Mao, X. Dong, X. Jia, F. Zhang, F. Zhang, F. Yang, Z. Wang, Q. Peng, Y. Shi, J. Hu, T. Xiang, X. Chen, Z. Wu, C. Chen, and X. J. Zhou, *Orbital origin of extremely anisotropic superconducting gap in nematic phase of FeSe superconductor*, Physical Review X **8**, 031033 (2018).
- [44] T. Okada, Y. Imai, K. Kitagawa, K. Matsubayashi, M. Nakajima, A. Iyo, Y. Uwatoko, H. Eisaki, and A. Maeda, *Superconducting-Gap Anisotropy of Iron Pnictides Investigated via Combinatorial Microwave Measurements*, Sci Rep **10**, 7064 (2020).